

# PERFORMANCE EVALUATION OF BITUMINOUS MIXES

---

---

### 7.1 Preamble

All bituminous mixes suffer deterioration over time due to the traffic movement and exposure to various environmental conditions. These deteriorations can manifest in the mixes in the form of distresses like rutting, fatigue cracking, low temperature cracking, moisture susceptibility, and ravelling, etc. The influence of type and quantity of fillers on the performance of bituminous mixes (prepared at OBC), for various distresses, was investigated using suitable testing protocols. In addition to this, the section also analyzed the effect of fillers on the behavior of bituminous mixes against long-term ageing with ageing index determined corresponding to various parameters (Marshall stability, Marshall Quotient, indirect tensile strength, tensile strength ratio, Cantabro loss). Finally, the resilient modulus of mixes was also examined to analyze the load distribution behavior of bituminous mixes and calculation of pavement layer thicknesses in subsequent chapter. Various correlations between mastics and mix properties were also been established in this chapter.

### 7.2 Rutting Resistance

The rutting of bituminous mixes is considered to be one of the primary modes of failure in bituminous pavements. Pavements with thick bituminous layers display substantial rutting in bituminous layers, especially at high temperatures, lower speeds, and heavy traffic conditions. In this study, the rutting resistance of various mixes was evaluated using Marshall Quotient and static creep tests.

### **7.2.1 Marshall Quotient**

Marshall Quotient (MQ), also known as rigidity ratio, is defined as the ratio of Marshall stability (kN) to flow (mm) value of compacted Marshall specimen at failure. It is a well-recognized criterion used by various researchers to assess the rutting resistance of bituminous mixes (Arabani et al., 2017; Bostancioğlu and Oruç, 2016; Moghaddam et al., 2014; Whiteoak 1991). Bituminous mix having MQ value displays superior stiffness as well as better load distribution capability, which ultimately results in its improved resistance against creep or rutting. In Indian specification (MoRTH, 2013), a range of Marshall quotient (2-5 kN/mm) is specified to design rut resistant as well as to avoid excessive brittle bituminous concrete mixes. A total of 48 specimens (3 for each mix) were prepared at OBC according to MS-2 guidelines, whose details are explained in Chapter 5. The MQ values of all mixes were determined at 60°C, and average values are reported in Figure 7.1.

### **7.2.2 Static Creep and Recovery Test**

The rutting resistance of bituminous mixes was also determined using uni-axial static creep and recovery test. This test is inexpensive and easy to conduct, and used by several researchers (Chandra and Choudhary, 2013; Diab and Enieb; 2018; Kuity et al., 2014). The rutting in the bituminous mixes depends upon the effect of loading and unloading. The mechanism of static creep and recovery test considers the impact of vehicle tyre on the pavement surface. It involves the application of a uni-axial static load on a standard Marshall specimen for a specific time and temperature, and measurement of its axial deformation. When a static load is applied to the Marshall specimen over a period of time, the specimen undergoes deformation. Due to the viscoelastic nature of bitumen and bituminous mix, a part of this deformation recovers

in period of time after load is removed from the specimen. The non-recoverable (permanent) deformation of the mix is termed as creep deformation, which could be used as a parameter of its rutting resistance. The higher the permanent deformation, the lower is rutting resistance of the mix and vice versa.

This test was conducted as per the BS 598: Part 111 (1995) guideline. The load set up was fabricated in the laboratory in which a constant load was applied to the Marshall specimen to generate an axial stress of 100 kPa, for a loading time period of 60 minutes at an ambient temperature of  $35\pm 2^{\circ}\text{C}$ . After setting up the sample, a conditioning load was applied, which provided a stress equivalent to 10 kPa for 10 minutes, and any axial deformation during this period was ignored. After 10 minutes, the load was increased to the test load, and axial deformations were measured throughout the test period, with dial gauges of 0.001 mm least count. The readings were taken at 10, 30, 60, 120, 180, 240, 300, 600, 900, 1200, 1500, 1800, 2100, 2400, 2700, 3000, 3600 seconds. After an hour of loading, the load was removed and the recoverable part of deformation was recorded for next half an hour at regular intervals of 5 minutes each. The graph of axial deformation versus time is plotted and the final permanent deformation is determined to assess the rutting performance of bituminous mix. The deformation versus time curves for all mixes are shown in Figure 7.2, and average permanent deformation is reported in Table 7.1.

### **7.2.3 Analysis of Rutting Resistance**

The MQ values of the mixes are stated in Figure 7.1. It can be seen that the MQ values for all mixes increased with the filler content. This trend is in agreement with the results obtained in previous studies (Chandra and Choudhary, 2013; Sharma et al.,

2010). In general, it is observed that mixes with lower VMA and apparent film thickness (AFT) resulted in higher MQ values and vice versa (Christenson and Bonaquist, 2006; Jenks et al., 2011). The relationship between the MQ and VMA as well as between MQ and AFT was explored and consistent trends were found (Figure 7.3 (a) and (b)). Since both VMA and AFT of mixes decreased with filler contents, MQ values were also found to increase. The relationship between the rutting resistance of the mixes and mastics was also explored. A plot between the MQ values of mixes and Superpave rutting parameter ( $G^*/\sin\delta$ ) of mastics at 64°C was drawn, and a decent trend is observed (Figure 7.3(c)). Similarly, a plot between the MQ values of mixes and  $J_{nr}$  values of mastics at 3.2 kPa stress was determined at 64°C, which also found a consistent trend (Figure 7.3(d)). However, MQ values were strongly related to the properties of mixes (higher  $R^2$  values) rather than of mastics.

In general, the mixes containing GL fillers displayed the highest MQ values followed by KS, GP, and conventional SD mixes. However, there are some exceptions, such as, at 8.5% filler, SD mix displayed relatively higher MQ than GP mix. The testing of MQ values was done at 60°C temperature, which was achieved by placing the specimens into water bath for 30 minutes. Unlike SD, which consisted of dolomite (ensure strong bitumen-filler bonding), GP predominately consisted of silica and there was a possibility of loosening of bond between bitumen and filler in the presence of water (Pasandin et al., 2016; Wu et al., 2007). This might have resulted in slight lower rate of increase in MQ values with filler content in comparison SD mix.

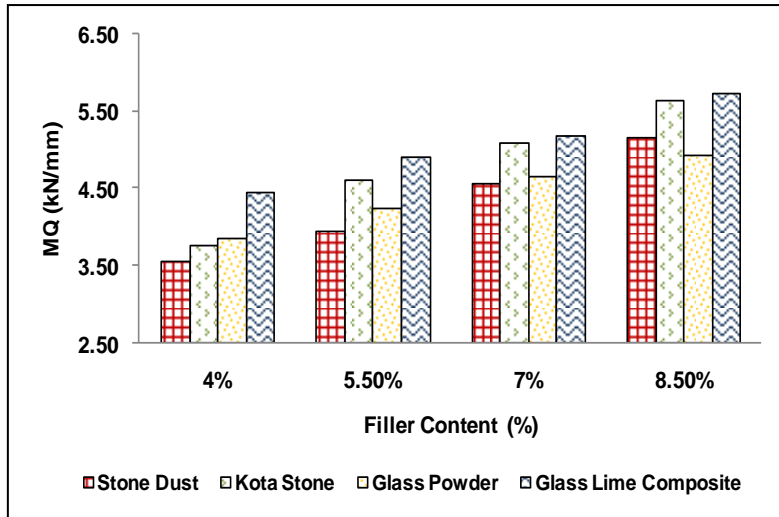
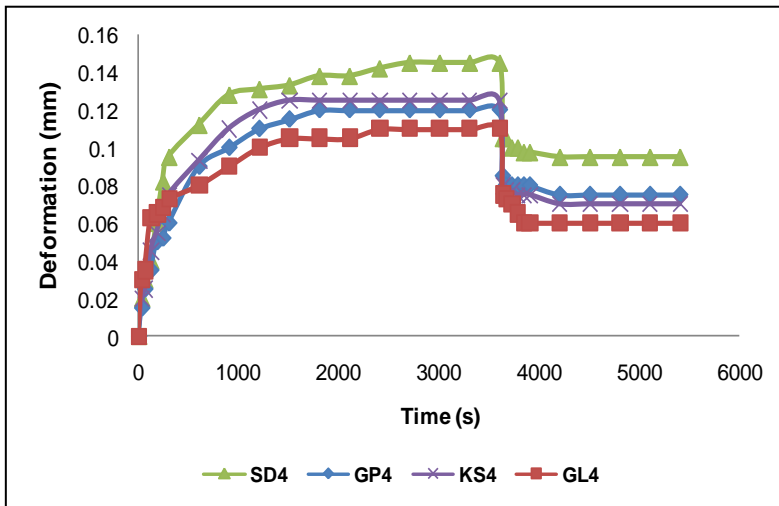
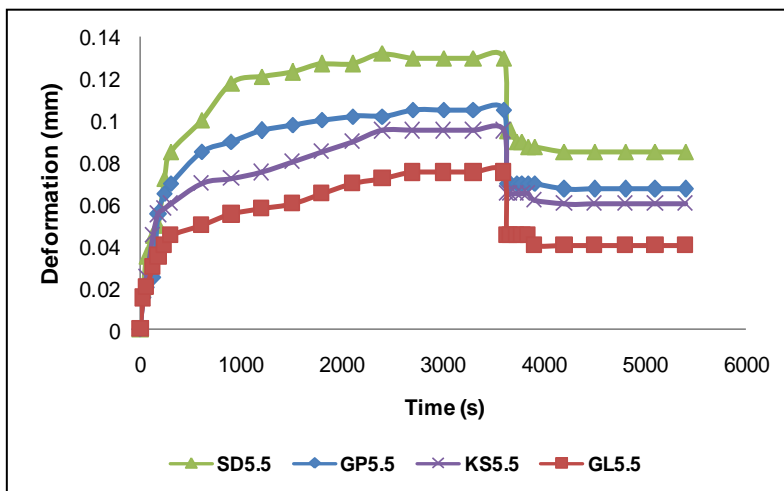


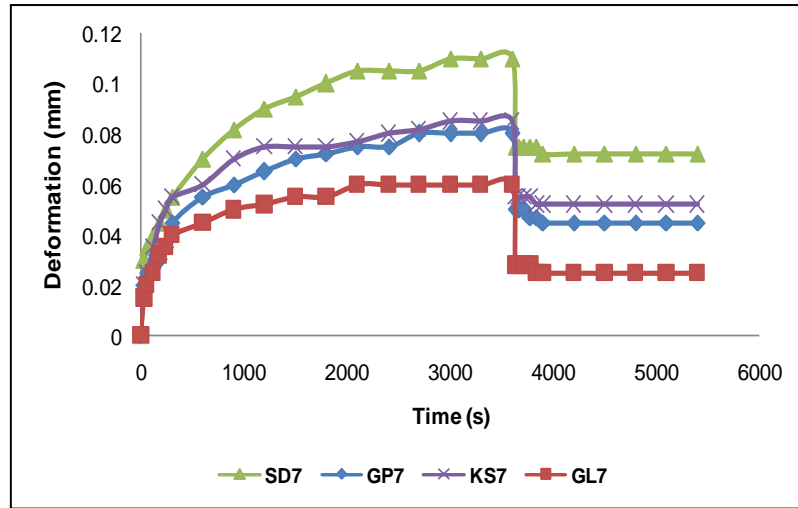
Figure 7.1 Marshall quotient values of various mixes



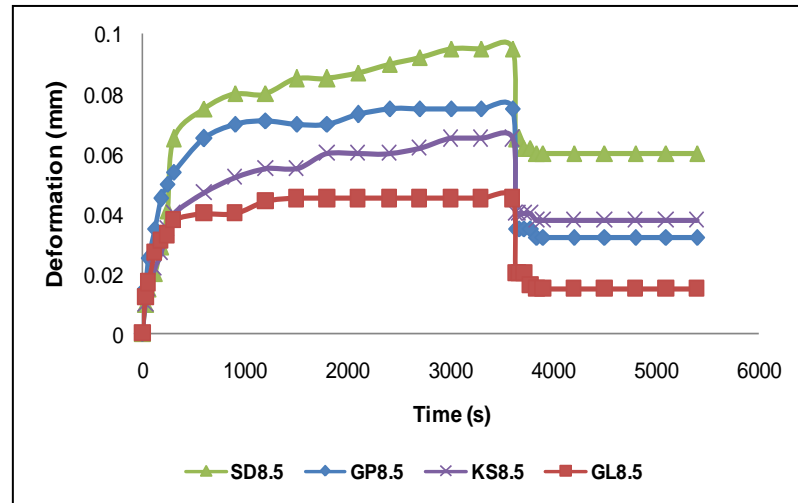
(a) Deformation versus time curves for the mixes having 4% filler



(b) Deformation versus time curves for the mixes having 5.5% filler

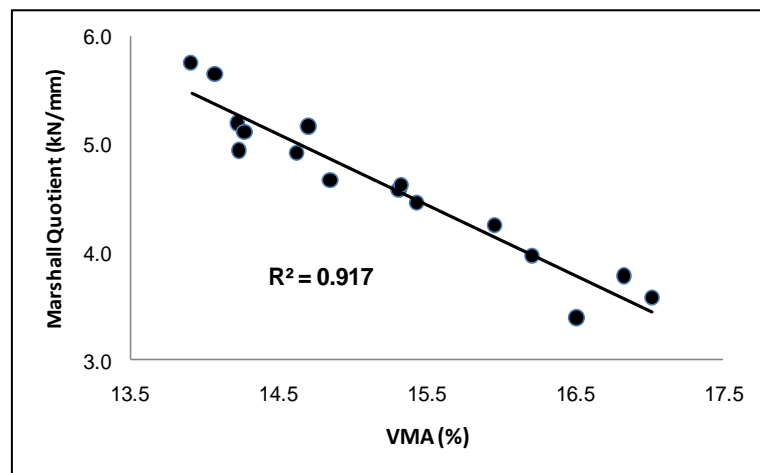


(c) Deformation versus time curves for the mixes having 7% filler

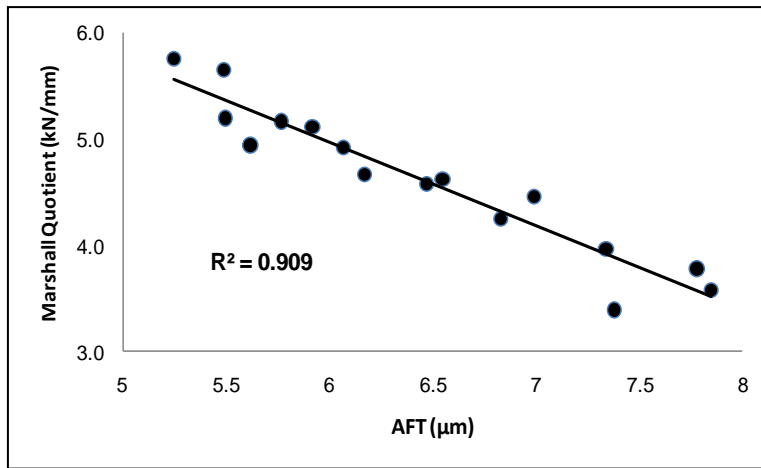


(d) Deformation versus time curves for the mixes having 8.5% filler

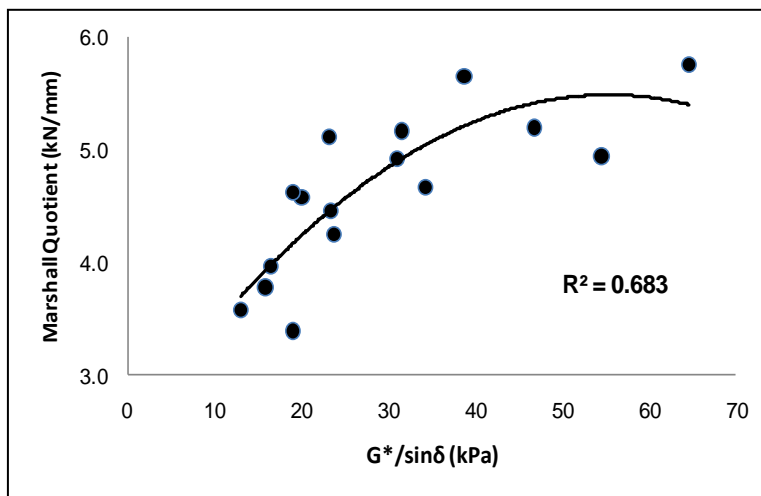
Figure 7.2 Deformation versus time curves of various mixes



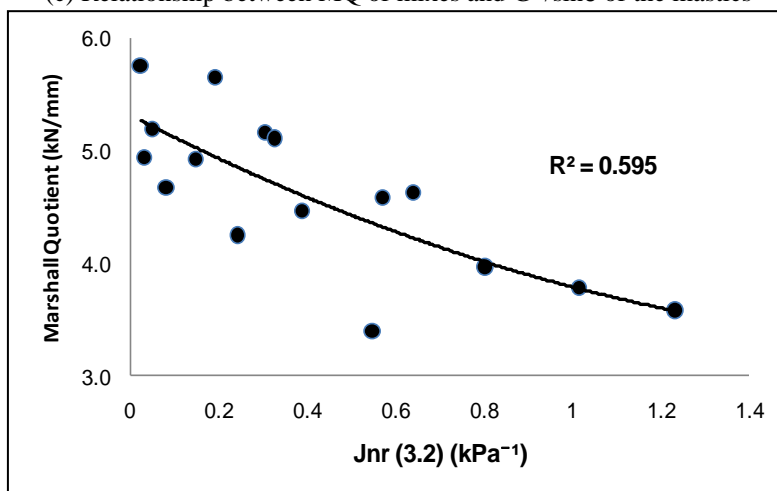
(a) Relationship between MQ and VMA of the mixes



(b) Relationship between MQ and AFT of the mixes

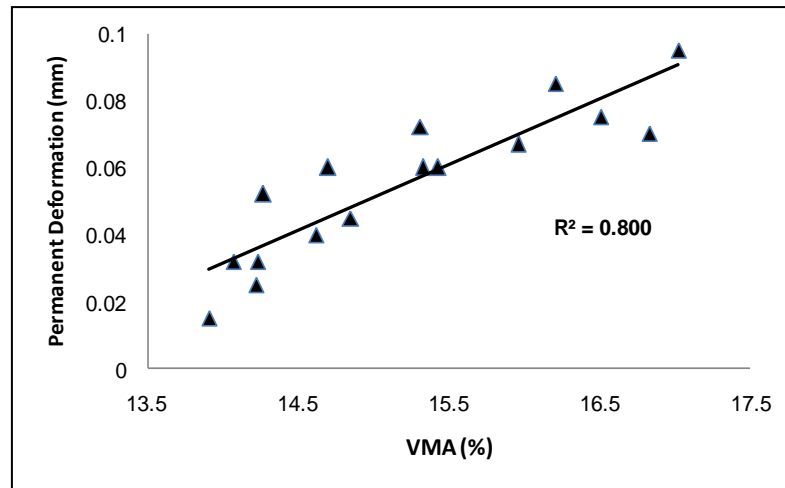


(c) Relationship between MQ of mixes and  $G^*/\sin\delta$  of the mastics

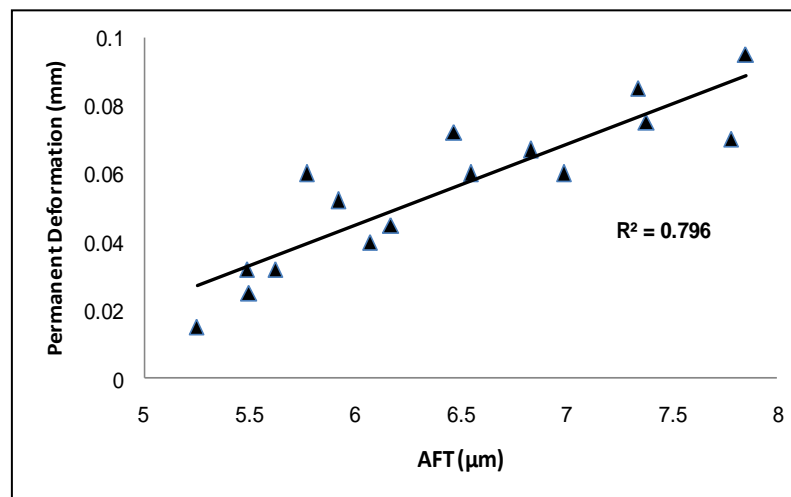


(d) Relationship between MQ of mixes and  $J_{nr}$  (3.2 kPa) of the mastics

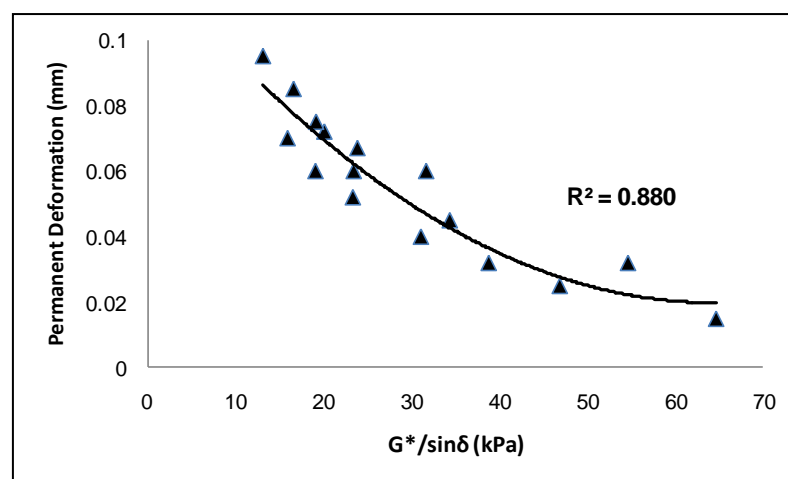
Figure 7.3 Relationship between MQ and various mixes and mastic parameters



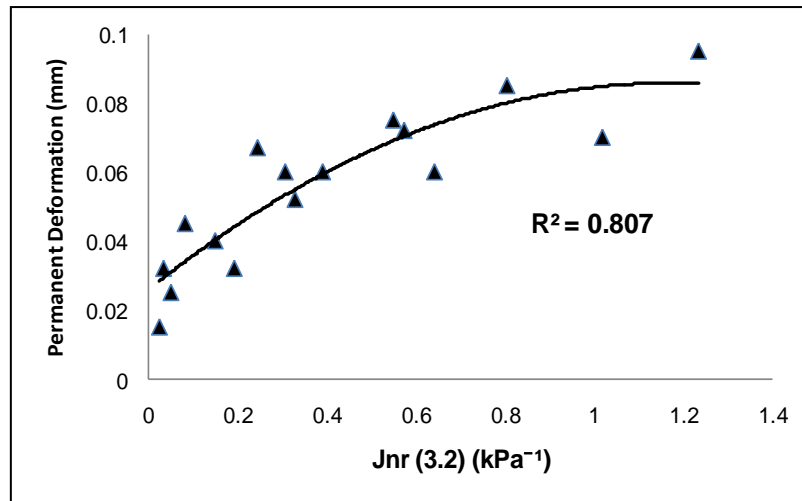
(a) Relationship between permanent deformation and VMA of the mixes



(b) Relationship between permanent deformation and AFT of the mixes

(c) Relationship between permanent deformation of mixes and  $G^*/\sin\delta$  of the mastics





(d) Relationship between permanent deformation of mixes and  $J_{nr}$  (3.2 kPa) of mastics

Figure 7.4 Relationship between permanent deformation in mixes and various mixes and mastic parameters

In addition to MQ analysis, the relationship between rutting resistance of mixes and mastic parameters was also explored using static creep test. Similar to MQ values, the permanent deformation of the mixes was found to decrease with the increase in filler content (Figure 7.2). Similarly, strong correlations were observed between the permanent deformation of mixes and their VMA and AFT ((Figure 7.4 (a) and (b)). In comparison to the MQ values, the correlations between the permanent deformation and the mastic properties ( $G^*/\sin\delta$  and  $J_{nr}$ ) were found to be much stronger (Figure 7.4 (c) and (d)). It can be said that the static creep test displayed a better correlation with the mastic properties than MQ test. In general, GL mixes displayed the highest rutting resistance followed by GP, KS, and SD mixes. Static creep test was done at ambient temperature, without sample being exposed in water. Hence, unlike MQ test, GP mixes always exhibited superior rutting resistance than SD mixes at all filler concentrations. In conclusion, it can be said that increase in filler content tends to increase the rutting resistance of bituminous mixes and vice versa. The mixes containing waste fillers displayed superior rutting resistance than conventional SD mixes.

Table 7.1 Various parameters of bituminous mastic and mixes

Type of mix	MQ (kN/mm)	Permanent deformation (mm)	VMA (%)	AFT ( $\mu\text{m}$ )	$G^*/\sin\delta$ (kPa)	$J_{nr}$ (3.2 kPa) @ 64°C (kPa <sup>-1</sup> )
SD 4	3.6	0.095	17.0	7.85	13.09	1.234
SD 5.5	4.0	0.085	16.2	7.34	16.57	0.804
SD 7	4.6	0.072	15.3	6.47	20.07	0.573
SD 8.5	5.2	0.060	14.7	5.77	31.65	0.306
GP 4	3.4	0.075	16.5	7.38	19.13	0.549
GP 5.5	4.2	0.067	16.0	6.83	23.83	0.244
GP 7	4.7	0.045	14.9	6.17	34.33	0.081
GP 8.5	4.9	0.032	14.2	5.62	54.60	0.033
KS 4	3.8	0.070	16.8	7.78	15.89	1.018
KS 5.5	4.6	0.060	15.3	6.55	19.06	0.641
KS 7	5.1	0.052	14.3	5.92	23.31	0.328
KS 8.5	5.6	0.032	14.1	5.49	38.76	0.192
GL 4	4.5	0.060	15.4	6.99	23.41	0.390
GL 5.5	4.9	0.040	14.6	6.07	31.05	0.149
GL 7	5.2	0.025	14.2	5.50	46.84	0.048
GL 8.5	5.7	0.015	13.9	5.25	64.62	0.024

### 7.3 Moisture Sensitivity

In bituminous mixes, the adhesive and cohesive forces between the aggregates and bitumen bonds different ingredients together as a single unit. The ingress of water from different sources (rainfall, ground water table, and water vapours) impairs the bond between bitumen aggregate interfaces and degrades the strength of the mix, which resulted in failure of pavement. Hence it is critical to ensure satisfactory moisture resistance of the bituminous mixes. In this study, the moisture sensitivity of various mixes was evaluated with the help of modified Lottman test and retained Marshall stability analysis.

### 7.3.1 Modified Lottman Test

The modified Lottman test (AASHTO T283) test prescribed by MoRTH (2013) was used to determine the moisture sensitivity of the bituminous mixes. As per the procedure, analysis of each type of mix requires six compacted Marshall (total of 96 specimens) having air voids in the range of  $7\pm 0.5$  percent. The level of air voids was maintained by adjusting the number of Marshall blows on each side by trial and error method.



(a) Partial vacuum saturation of specimen



(b) Packaging of specimens in plastic



(c) Specimens after being freeze for 16 hours

Plate 7.1 Conditioning of specimens in modified Lottman test

These six specimens were divided into two sets of three specimens each. First set was referred to as the unconditioned set, while the other was subjected to a freeze-thaw cycle and referred to as conditioned specimens. The conditioned specimens were placed in a vacuum container completely submerged in water, and a vacuum of

absolute pressure of 13-67 kPa is applied for 15 minutes (Plate 7.1(a)). This was done to ensure that the volume of water in the specimen should be 55 and 80% of the total volume of air. After saturation, the samples were tightly wrapped in plastic sheets and were placed in a freezer maintained at  $-18 \pm 3^\circ\text{C}$  for 16 h (Plate 7.1(b) and (c)). The specimens were then removed from the freezer and were placed in a water bath maintained at  $60 \pm 0.5^\circ\text{C}$  for 24 h. Finally, the specimens were removed from the water bath, and they, along with unconditioned specimens, were kept in another water bath maintained at  $25 \pm 0.5^\circ\text{C}$  for 2 h. The indirect tensile strength of both unconditioned and conditioned set of specimens is determined at  $25^\circ\text{C}$ . The indirect tensile strength of the specimens was calculated as per ASTM D6931 procedure (details are discussed in subsequent sections) using Equation 7.1.

$$ITS = \frac{2000P_{max}}{\pi DT} \quad [7.1]$$

Where,  $ITS$  = Indirect tensile strength (kPa)

$P_{max}$  = Maximum applied load (N)

$D$  = Diameter of specimen (mm)

$T$  = Thickness of specimen (mm)

The moisture sensitivity of mixes was determined in term of tensile strength ratio (TSR) which was calculated as:

$$TSR = \frac{ITS_{cond}}{ITS_{uncond}} \times 100 \quad [7.2]$$

Where,  $TSR$  = Tensile strength ratio (%)

$ITS_{cond}$  = Indirect tensile strength of conditioned specimen (kPa)

$ITS_{uncond}$  = Indirect tensile strength of unconditioned specimen (kPa)

According to MoRTH (2013), the bituminous mixes should have minimum TSR value of 80% to ensure satisfactory moisture resistance.

### 7.3.2 Retained Marshall Stability Test

In addition to the modified Lottman test, the durability of bituminous mixes against moisture was also determined using the retained Marshall stability test. This test is not a part of the current Indian specification (MoRTH, 2013), although it was specified in MoRTH (2001) specification. It is a relatively simple test than modified Lottman and requires lesser time and resources to perform. In this test, for each type of mix, six compacted Marshall specimens with 4% air voids and OBC were prepared and were divided into two groups having three specimens each. Specimens in group I was referred to as conditioned specimens, and were subjected to water conditioning by immersing them in a water bath maintained at 60°C for a period of 24 hours. On the other hand, specimens of group II were referred to as unconditioned specimens and were normally immersed in water bath for 30 minutes maintained at a temperature of 60°C. The average stability values for each group were calculated, and the retained Marshall stability were reported in the form of percentage as per Equation 7.3

$$RMS = \frac{MS_{cond}}{MS_{uncond}} \times 100 \quad [7.3]$$

Where,  $RMS$  = Retained Marshall stability(%)

$MS_{cond}$  = Marshall stability of conditioned specimen (kPa)

$MS_{uncond}$  = Marshall stability of unconditioned specimen(kPa)

According to MoRTH (2001), the bituminous mixes should have minimum RMS value of 75% to ensure satisfactory moisture resistance.

### 7.3.3 Analysis of Moisture Sensitivity

The TSR and RMS values of the various mixes are stated in Table 7.2. Although RMS values of mixes were found to be slightly higher than TSR values, they exhibited a good relationship (Figure 7.5). Mixes having higher TSR and RMS values said to display superior moisture resistance. Both TSR and RMS values of bituminous mixes decreased with the increase in filler content. It implied that the moisture sensitivity of the bituminous mixes increased with the increase in filler content. The apparent film of bitumen acts as a protective layer to ensure satisfactory durability of bituminous mixes against moisture. Due to decrease in OBC of the mixes, AFT of bitumen also decreased with the increase in filler content, which resulted in decline of moisture resistance of the mixes (Sengoz and Agar, 2007). The observed trend was found similar to the results observed in previous studies (Chandra and Choudhary, 2013; Huang et al., 2007; Sharma et al., 2010).

The conventional SD and KS mix displayed superior moisture resistance at all filler contents and had highest TSR and RMS values. SD and KS mixes displayed good moisture resistance due to the presence of dolomite ( $\text{CaMg}(\text{CO}_3)_2$ ) and calcite ( $\text{CaCO}_3$ ) in the composition of SD and KS, which maintain good adhesion in between bitumen and filler even in the presence of water (Pasandin et al., 2016). However, KS has higher active clay content than SD as determined from their methylene blue values in Chapter 4, hence KS mixes had marginally lower TSR and RMS values than SD mixes. Lower moisture susceptibility of KS mixes might also be due to their lower AFT than SD mixes. GP mixes displayed inferior performance against moisture, and failed to fulfill criteria of minimum TSR (80%) at any filler content. However, GP mixes prepared at 4% fulfilled the minimum criteria of RMS (75%). Hence, GP

modified mixes are expecting to perform poorly in the region subjected to freezing-thawing conditions. This may be due to weak bond in bitumen-aggregate caused by the predominance of silica in the GP, and a few previous studies have also observed the similar results (Sanij et al., 2019; Wu et al., 2007). However, it was found that replacement of 2% glass powder with hydrated lime (HL) had dramatically improved the values of TSR and RMS. The improvement in performance is attributed to the anti-stripping nature of HL caused due to the presence of calcium-based water-insoluble minerals like Portlandite ( $\text{Ca}(\text{OH})_2$ ) in its composition (Lesueur et al., 2013; Pasandin et al., 2016). GL mixes displayed significantly high TSR values than GP mixes and have shown satisfactory TSR up to 7% of filler content in the mix. Hence, it can be said that up to 5% of GP along with 2% of HL can be satisfactorily be utilized as a filler.

Table 7.2 RMS and TSR values of various mixes

Filler content (%)	Stone dust		Kota stone		Glass powder		Glass – hydrated lime	
	RMS (%)	TSR (%)	RMS (%)	TSR (%)	RMS (%)	TSR (%)	RMS (%)	TSR (%)
4.0	93.19	94.23	96.41	97.89	77.89	54.05	92.52	88.58
5.5	92.31	93.28	91.74	91.34	69.74	39.47	91.24	85.34
7.0	90.24	89.26	88.84	86.65	62.21	17.65	89.79	81.12
8.5	88.57	85.59	84.62	83.87	56.58	09.18	85.25	71.27

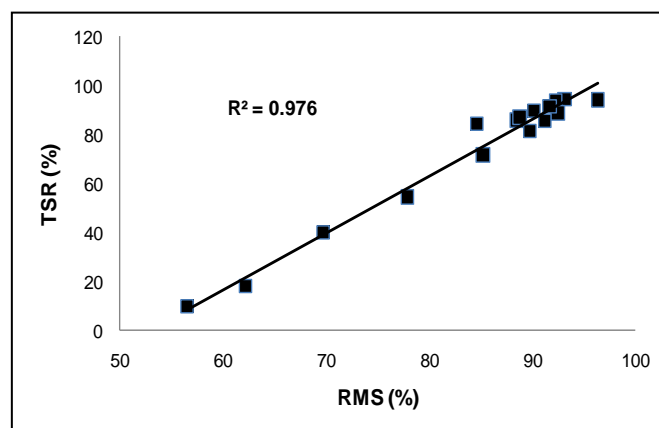


Figure 7.5 Relationship between RMS and TSR of various mixes



Plate 7.2 Untested GP 8.5% mix after being subjected to freeze-thaw conditioning

## 7.4 Adhesion Analysis

Adhesion is the tendency of dissimilar molecules to maintain intimate contact (Miller et al., 2012). Good adhesion between bitumen and aggregates in the bituminous mix in a dry state, as well as in the presence of water is crucial for its satisfactory performance and durability (Bhasin and Little, 2009). The loss of adhesion in the aggregate-bitumen interface is one of the primarily responsible mechanisms for high moisture susceptibility in the mixes. It could be divided into two components, namely active and passive adhesion.

### 7.4.1 Active Adhesion

The bitumen's ability to completely cover the aggregates during the mixing operation of bituminous mixes can be termed as its active adhesion (Cui et al., 2019; Pasandin and Perez, 2015). It's a function of not only the materials' surface energies, but also the mixture/binder viscosity, and applied shear forces during mixing. Active adhesion can also be represented by the term mixability. The effect of various fillers on the active adhesion was analyzed by measuring the time required by the aggregates in the mix to get uniformly coated with the bitumen (Pasandin and Perez, 2015). The mixing of all ingredients was done at the mixing temperature of the bituminous mix. The



mixing time is the total time (in seconds) elapsed between the moment of the binder addition into the mix and the moment at which all aggregates in the mix achieve 100% coating (Pasandin and Perez, 2015).

#### **7.4.2 Passive Adhesion**

Passive adhesion can be defined as the ability of bitumen to remain on the aggregate surface when it is subjected to the external agents like traffic and moisture (Cui et al., 2019; Pasandin and Perez, 2015; Tarrer and Wagh, 1991). Passive adhesion analysis was done as per ASTM D3625-12 (2005) specification. For each mix, loose sample weighing 250 g is prepared at the mixing temperatures and then cooled to a temperature between 85°C and the boiling point of water (Plate 7.3). The sample is then placed into the container having boiling distilled water for 10 minutes. The bitumen that comes on the water surface was skimmed off, and the sample was cooled to room temperature (Plate 7.4). The sample was then removed from the water and placed on the white paper towel and visual observations of the degree of retained bitumen coating were conducted by the team of 5 people and reported in terms of percentage (Plate 7.5).

#### **7.4.3 Analysis of Active and Passive Adhesion**

Results of active and passive adhesion analysis are stated in Figures 7.6 and 7.7. Bituminous mixes with lower mixing time and retained bitumen coverage have superior active and passive adhesion, respectively. Similar to TSR values, SD and KS mixes displayed superior active and passive adhesion followed by GL and GP mixes, respectively. SD and KS mixes had the least mixing time and highest bitumen coverage than GL and GP mixes respectively. The higher alkaline nature of SD may

be responsible for their good adhesion with bitumen than KS mixes. Other than that, the higher OBC of SD mixes might also be a responsible factor for their superior active and passive adhesion than KS mixes. Alkaline nature of SD and KS may be responsible for their good adhesion with bitumen. GP modified mix was found to have the worst active and passive adhesion values due to their high silica content. A few previous studies on the glass-based aggregates and fillers also have verified the poor moisture resistance of their mixes (Sanij et al., 2019; Wu et al., 2007).



Plate 7.3 Measuring temperature of loose mix



Plate 7.4 Skimming of free bitumen from top surface of boiled water



Plate 7.5 Analysis of stripping by visual inspection

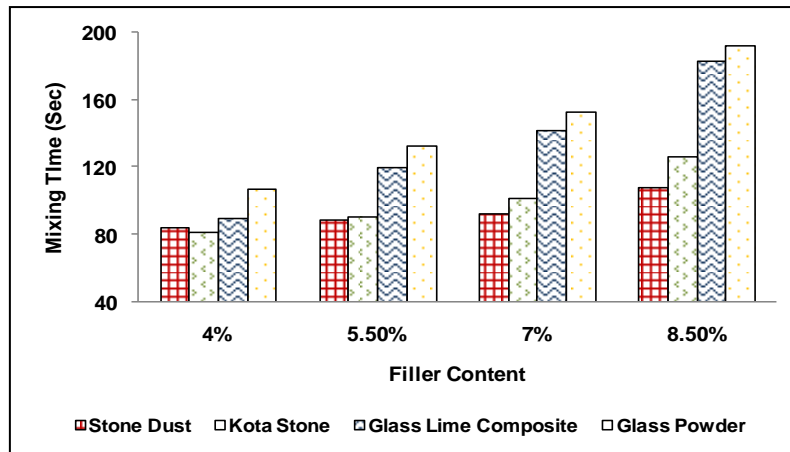


Figure 7.6 Effect of filler content on mixing time of bituminous mixes

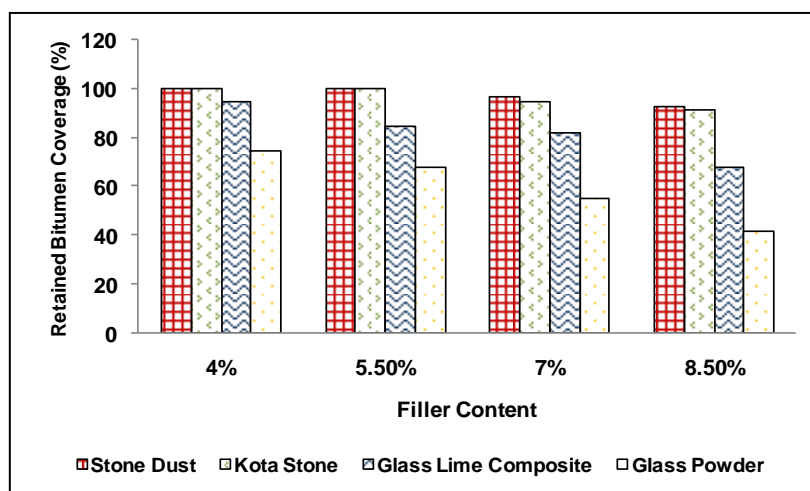


Figure 7.7 Effect of filler content on retained bitumen coverage of bituminous mixes

Both active and passive adhesion values decreased with the increase in filler content. SD and KS didn't significantly influence the active and passive adhesion of the mixes, especially at lower filler concentration (4 and 5.5%). Even GL mixes have displayed almost similar performance as SD and KS mixes at 4% content, which may be due to the adhesion promoter behavior of hydrated lime. However, this influence seemed to diminish at higher filler contents (7% and 8.5%), and GL mixes delivered performance almost similar to GP mixes. It can be inferred that the influence of filler is noticeable at the higher filler concentration than at mixes with lower filler concentration.

## **7.5 Cracking Resistance**

The temperature sensitive nature of bituminous mixes led to the formation of thermal cracks (low, intermediate temperature cracking and fatigue cracking), which deteriorate the pavement performance. Cracking at lower temperatures is observed due to sudden drop in temperature induced tensile stress in combination with embrittlement of the bituminous concrete (Christensen and Bonaquist, 2004). Fatigue cracking initiates at the bottom of the surface layer of bituminous mixes due to the tensile stresses induced by traffic loading at intermediate temperatures (Al-Khateeb et al., 2008; Nguyen et al., 2013). Hence, the tensile strength of the bituminous mix is related to its thermal cracking (Si et al., 2016). The cracking resistant behavior of bituminous mixes has been widely analyzed using indirect tensile strength test. The mixes having higher indirect tensile strength correspond to higher thermal cracking resistance (Bennart et al., 2018; Christensen and Bonaquist, 2004; Si et al., 2016). Indirect tensile strength is also an important parameter needed for the determination of resilient modulus and fatigue life of the mixes using test methods, which involves the application of test loading along the diametrical axis.

### **7.5.1 Indirect Tensile Strength**

In this study, the indirect tensile strength (ITS) of bituminous concrete mix was determined according to ASTM D 6931 guideline. This evaluation was performed at 25°C and 0°C to investigate the performance of the mixes at intermediate and low temperatures. In this test, a compressive force was diametrically imposed on a standard Marshall sample (4% air voids) with the help of steel strips at a constant rate of 50.8 mm/min (Figure 7.8).

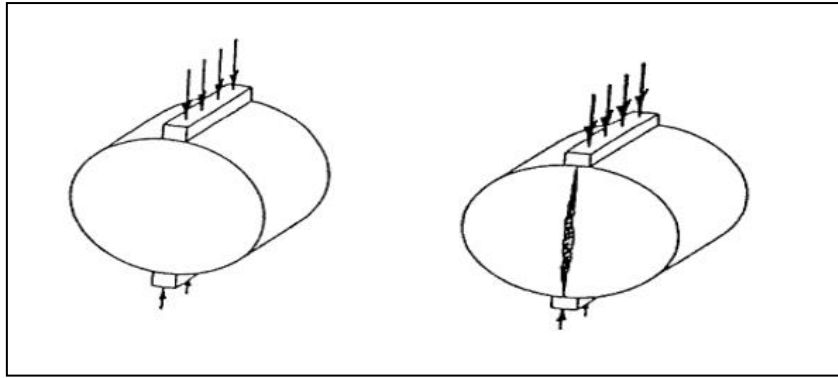


Figure 7.8 Line diagram showing loading set up of ITS determination (Bindu, 2012)

The maximum load sustained by the specimen was used to calculate the indirect tensile strength with the Equation 7.4. The higher *ITS* values of the mix correspond to its better cracking resistance and vice versa (Bennart et al., 2018; Christensen and Bonaquist, 2004; Si et al., 2016).

The *ITS* values were determined using the Equation 7.4

$$ITS = \frac{2000P_{max}}{\pi DT} \quad [7.4]$$

Where, *ITS* = Indirect tensile strength (kPa)

$P_{max}$  = Maximum applied load (N)

*D* = Diameter of specimen (mm)

*T* = Thickness of specimen (mm)

### 7.5.2 Analysis of Indirect Tensile Strength at Different Temperatures

The indirect tensile strength of mixes at 25°C and 0°C are shown in Figures 7.9 and 7.10, respectively. At both temperatures, *ITS* values of the mixes were found to increase with the filler content irrespective of the type of filler. It is already established that aggregates in the bituminous mixes are bound together with the virtue of mastic, which is a composite material made of bitumen and filler. Hence, the improvement of *ITS* with filler content can be explained with the principle of

composite mechanics. Understandably, the filler has a higher strength than the bitumen. So, at higher filler content, an increase in the portion of filler and a simultaneous decrease in bitumen content in mastic will inevitably increase the strength of mastic as well as ITS values of the bituminous mixes (Diab and Enieb, 2018; Huang et al., 2007). Increase in the filler content in mixes also increased the density of mixes, which might also be a possible reason for its increase in ITS values (Diab and Enieb, 2018).

Similar to the rutting resistance, the mixes containing waste fillers displayed superior ITS than conventional SD mixes. GL and SD mixes clearly displayed the maximum and minimum ITS values at all filler levels. GP mixes displayed higher ITS values than KS mixes at 4% filler concentration. However for the mixes prepared at intermediate and higher filler concentrations (4-8.5%), KS mixes displayed marginally higher ITS values. The increase in the volume fraction of filler tends to increase the stiffness of the mastic and mixes, and thus improved the ITS. Since GL and GP occupied the highest volume, they exhibited higher ITS values than conventional SD mixes. However, few studies have observed that finer fillers have a great potential for uniform distribution and formation of an integrated structure in the bituminous mix, which ultimately improves the ITS of the mixes (Modarres and Bengar, 2017; Modarres and Rahmanzadeh, 2015). In chapter 4, it has already been established that KS is much finer filler than GP as it displayed lower fineness modulus and  $D_{50}$  values. Hence, KS seemed to distribute more uniformly than GP, and its mixes displayed higher ITS values than GP mixes. KS also displayed better bonding with bitumen and has superior ability to cement aggregates in the mixes than GP, which might also be a possible reason for superior ITS values of its mixes. ITS

values of the mixes at 0°C followed almost an identical trend as mixes at 25°C. However, considerable growth in ITS values is clearly observed with the drop in the testing temperature. This trend is found similar to that observed in some studies (Si et al., 2016; Vasconcelos et al., 2012). It was attributed to the higher stiffening of bitumen due to its increase in elastic nature with the decrease in temperature. Hence GL mixes displayed the highest low temperature cracking resistance followed by KS, GP, and SD mixes.

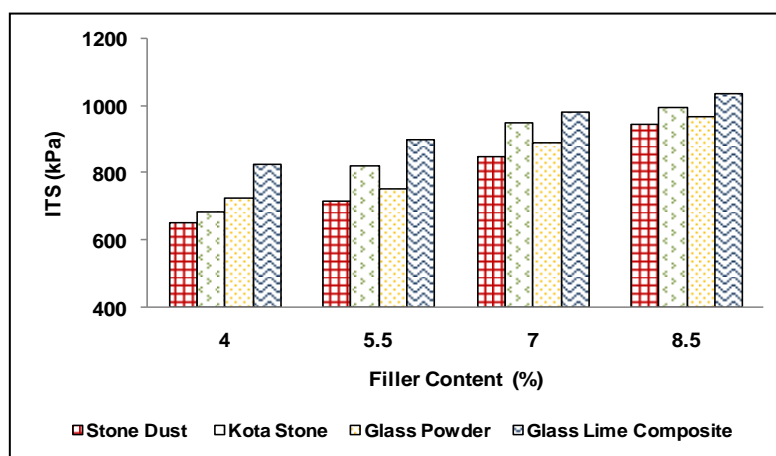


Figure 7.9 Variation of indirect tensile strength of mixes at 25°C with filler content

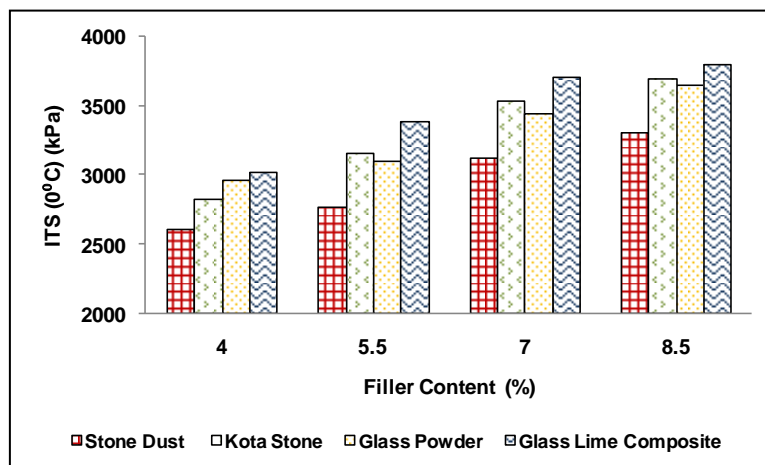


Figure 7.10 Variation of indirect tensile strength of mixes at 0°C with filler content

## **7.6 Fatigue Resistance**

The fatigue is one of the primary modes of failure in bituminous layers, which manifests itself in the form of cracking due to the repeated traffic loading. The repeated loading of the bituminous layer with every passage of vehicle results in the reduction of the stiffness of the bituminous mix and its subsequent accumulation with time may lead to complete failure (Di Benedetto et al., 2004; Saboo, 2015). Fatigue failure is a three-stage process that initiates the development of micro-cracks at bottom of the bituminous layer. These micro-cracks coalesce to form macro-cracks, which finally propagate upwards to the surface and appear in the form of alligator cracking that causes disintegration of the pavements.

The testing methods to determine fatigue resistance can be classified into two modes according to their loading behavior, as stress (controlled–stress) and constant strain (controlled–strain) mode of testing. The significance and advantages of various test methods have already been discussed in detail during the review of the literature of this study (Chapter 2). In this study, the fatigue resistance of bituminous mixes is determined using indirect tensile fatigue test (ITFT) at constant stress mode. Due to unavailability of the testing facility at the parent institution, the specimens were prepared at the parent institute, but were tested in the pavement engineering laboratory of IIT (Kharagpur), India. ITFT method was used to determine the fatigue resistance since it offers following advantages over other methods (Monismith et al., 1990; Smith, 2001; Tangella et al., 1990)

- (a) It is simple in nature
- (b) Failure is initiated in a region of relatively uniform tensile stress



(c) A biaxial state of stress exists, possibly of a type better representing field conditions.

(d) Standard Marshall specimens are used in testing which can be manufactured easily without any sophisticated equipments.

(e) Testing time is much lower than constant strain test methods

(f) The same testing equipment can be used for other tests such as resilient modulus and indirect tensile strength test.

The details of test methods are explained below.

### **7.6.1 Indirect Tensile Fatigue Test (ITFT)**

The ITFT was performed at 25°C for the prediction of fatigue life of various mixes as per EN 12697-24 specification with universal testing machine (UTM 14) (Plate 7.6).

The machine was equipped with a temperature control chamber that maintains a constant temperature during specimen conditioning and testing. The chamber was also equipped with two linear variable differential transducers to measure the skin and core temperatures of the specimens. All specimens were conditioned in the chamber for 24 h to achieve targeted testing temperature (25°C) (Plate 7.7). The test was conducted under controlled stress conditions with a load corresponding to stress level equal to 40% of the indirect tensile strength of the compacted Marshall specimen (with 4% air voids) (Modarres and Bengar, 2017; Bocci 2018; Gul et al., 2018). As per the clause E.4.1 of the EN 12697-24 specification, the test specimens should have fatigue life in the range between  $10^3$ - $10^5$  number of application. The fatigue life of all mixes tested at 40% stress level are found within this range and, hence stress level of 40% is finalized to limit the duration of the testing. The haversine load pulse with loading and rest periods of 0.1 s and 0.4 s, respectively, were as taken for the analysis. The

specimen was continuously loaded until its complete failure. Failure of specimen occurred when it collapsed, or its vertical deformation reached 9 mm, whichever happened first (Plate 7.8). The load repetition underwent by the specimen before its failure is considered as its fatigue life.

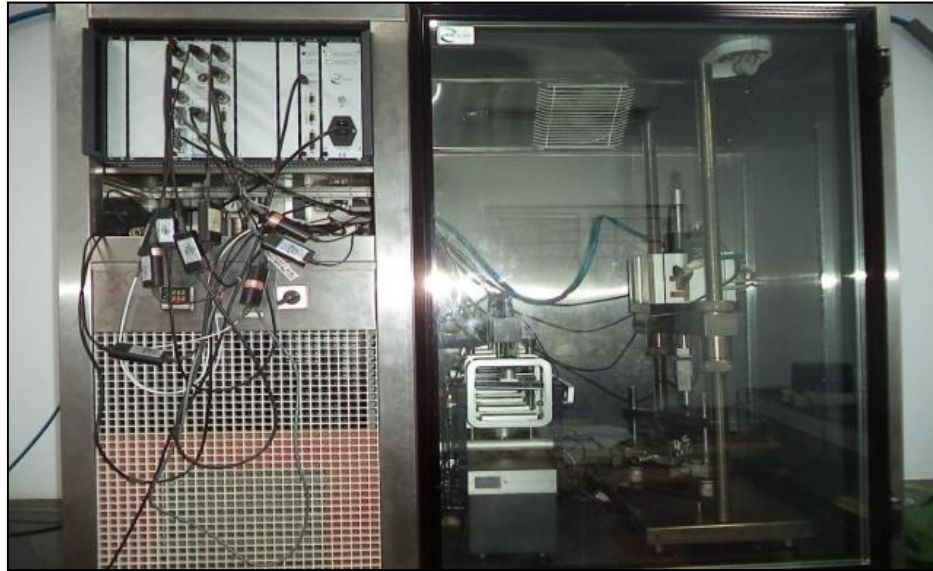


Plate 7.6 UTM-14 used in the testing of fatigue life of mixes

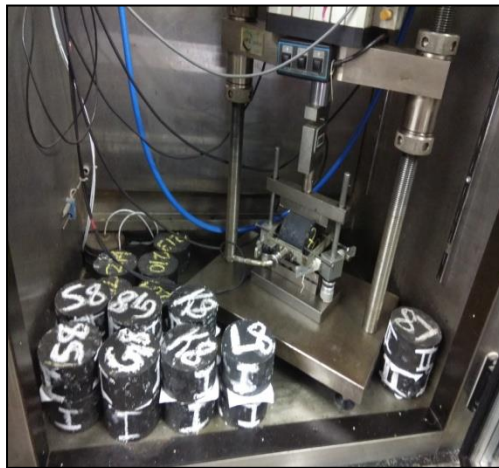


Plate 7.7 Conditioning of the specimens



Plate 7.8 Failure of a specimen

### 7.6.2 Fatigue Life Analysis of Bituminous Mixes

Result of fatigue live analysis at 40% stress level is shown in Figure 7.1. In general, fatigue lives of bituminous mixes increased with the filler content up to 7% of filler addition. However, the fatigue life of SD increased up to 8.5% of filler addition. The increase in fatigue life with the filler content might be attributed to the “crack

pinning” behavior of the filler. Crack pinning is the formal term given for the mechanism which suggested that the inclusions (in this case, filler) in a multiphase composite material (in this case, bitumen filler mastic) have an interaction which leads to slowing down of the growth of microcracks (Evans 1972; Smith and Hesp, 2000; Sobolev et al., 2014). It can be said that the filler particles in the mastic act as barriers that deflect the crack propagation (crack pinning) and thus enhance the fatigue lives of the mixes. The effect of type of filler on fatigue life is predominant at lower filler concentration (4 and 5.5%). However, the difference between the fatigue lives of different mixes diminished at higher filler concentrations (7 and 8.5%). GL and SD mixes displayed highest and lowest fatigue lives in most of the cases (except 8.5% filler). GP mixes displayed second highest fatigue lives at lower filler contents (4 and 5.5%), while KS mixes displayed second highest fatigue lives at higher filler concentration (7 and 8.5%).

The superior performance of mixes having waste fillers might be attributed to their lower specific gravity and fine particle size. Hydrated lime and GP have lowest specific gravity than SD, and hence they occupied larger volume in the bituminous mixes at a similar weight. Hydrated lime and KS are the finest filler, and their mixes also had lower OBC than SD mixes. Hence a higher volume of these fine filler acted as the barrier in the lower amount of bitumen, thus deflected the larger number of cracks and prolonged the fatigue lives. Finer filler particles also have a potential for uniform distribution and forming an integrated structure in the bituminous mix, which might have increased the fatigue life of the mixes (Modarres and Bengar, 2017).

Apart from the material properties, the mode of testing also influences the fatigue life of the mixes. Previous studies (Monismith et al., 1990; Smith, 2001) have suggested that the fatigue life of bituminous mixes increases with the increase in the stiffness of the mix, when testing is conducted in controlled stress mode. In this study, the testing was conducted in controlled stress mode, and the stiffness of mixes was found to increase with the filler content (Figure 7.1). Hence, the fatigue life was found to increase with the filler content (Monismith et al., 1990; Smith, 2001; Smith and Hesp, 2000). However, it must also be noted that fatigue life is also dependent on the bonding between the filler and bitumen. It has already been established that the bonding between bitumen and filler depends on the mineralogical composition of fillers. SD and KS fillers are made of calcium based alkaline minerals (dolomite and calcite) that form strong bond with bitumen. Hence they might have maintained their bond at higher filler concentration, which leads to the continual increase in fatigue life of SD mix and small drop of fatigue life in case of KS mix prepared at 8.5% filler. The hypothesis also seemed justifiable after observing the fatigue lives of GP and GL mixes at 8.5%. Here, GP mixes suffered a larger decline in fatigue life as compared to GL mixes, although both GP and GL have almost similar specific gravities. However since GL consist of 2% hydrated lime in its concentration; it prevented a higher decline in fatigue life of its mixes.

The performance of fatigue lives of mixes were compared with the fatigue resistance parameters of the mastics (Table 7.3). It can be inferred that none of the three mastic parameters followed the trend similar to that of the mixes. Hence based on the limited investigation, no strong correlation was found between the fatigue performance of mastics and mixes. However, out of the three mastic parameters, the percentage

elastic recovery (%R) determined at 3.2 kPa by MSCR test displayed a much closer trend with fatigue life of mixes. Both fatigue lives of the bituminous mixes and percentage recovery of mastics were found to increase with the filler content. On the other hand, fatigue resistance of mastics as per the Superpave fatigue parameter and LAS analysis was found to decrease with increase in filler content. The better correlation between %R and fatigue life of mixes might be due to the similar mode of testing. The fatigue life of the mixes was determined using ITFT performed at constant stress mode, while %R recovery of the mastic was also determined at a constant stress (3.2 kPa). Hence based on this limited investigation, it can be said that fatigue testing is strongly dependent on the mode of testing. This aspect can further be explored in detail for determining the fatigue life of mixes at constant strain mode of testing using methods such as four point beam bending test.

Table 7.3 Various fatigue parameters of bituminous mastics and mixes

Type of mix/mastic	Fatigue life of mixes (cycles)	$G^* \sin \delta$ (kPa)	Fatigue life of mastic at 2.5% strain (cycles)	Percentage recovery at 3.2 kPa stress (%)
SD 4	2491	1897	2368	65.42
SD 5.5	4201	3047	2156	67.25
SD 7	6036	3980	585	68.13
SD 8.5	6964	5294	230	70.24
GP 4	4324	3305	1282	70.92
GP 5.5	5932	4460	556	73.68
GP 7	6432	5878	217	79.40
GP 8.5	5321	6454	179	-
KS 4	3551	2813	2766	66.23
KS 5.5	5391	3809	1650	70.12
KS 7	7022	4445	477	68.92
KS 8.5	6481	6290	137	74.84
GL 4	4971	3950	855	72.75
GL 5.5	6326	6765	357	76.23
GL 7	7422	6856	179	87.13
GL 8.5	6886	7017	106	-

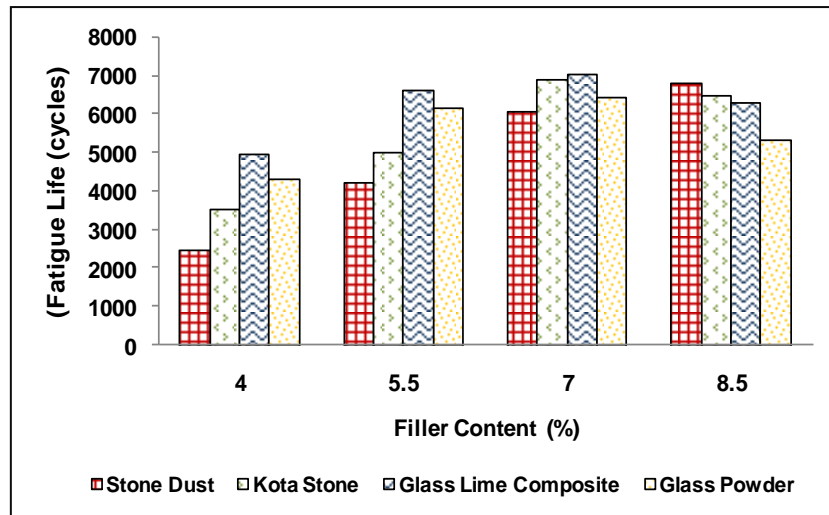


Figure 7.11 Variation of fatigue life of mixes with filler content

## 7.7 Ravelling Resistance

Ravelling can be termed as the progressive deterioration of bituminous surface layer from the surface downwards due to dislodgement of bitumen and aggregates. Ravelling, also known as abrasion failure, occurs at the stone-to-stone contact region in the mix due to loss of adhesion and cohesion in bituminous mastic (Zhang et al., 2018). The durability of bituminous mixes against ravelling can be determined using a simple procedure known as Cantabro test. Although it is traditionally used to assess the durability of open and gap-graded mixes, recent studies found the validity of test in cases of dense-graded mixes as well (Cox et al., 2017; Doyle and Howard, 2016; Kumari et al., 2018). Cantabro test measures the durability of the mixes against ravelling in the terms of loss of mass when it is subjected to the impact loading in Los Angeles abrasion machine. The detailed procedure of Cantabro test is stated below.

### 7.7.1 Cantabro Test

In this study, the ravelling resistance of the mixes was determined using two different kinds of Cantabro tests (standard and water immersion) as per Spanish norms NLT-352/86 (1986) and NLT-362/92 (1992), respectively. The standard test measures the

ravelling resistant of mixes without them being subjected to any conditioning (dry state). However, in the case of water immersion (wet) Cantabro test, the specimens were subjected to conditioning in water before being tested. It helped to analyze the effect of water on the ravelling of bituminous mixes.

For every mix, six standard Marshall specimens were prepared at OBC, which were divided into two groups each having three specimens. The first group was used to determine Cantabro loss in dry state. Three samples were placed in water bath maintained at 25°C for 24 hours. After 24 hours, the specimens were dried and their initial weight ( $W_1$ ) was recorded. Then each specimen was placed in Los Angeles abrasion testing machine without any abrasive charges and the machine was operated for 300 revolutions at a speed of 33 rpm. The weight of the specimen after testing ( $W_2$ ) was also recorded and percentage loss in weight of the specimen is recorded as abrasion loss. In case of the wet Cantabro test, the specimens in the second group were placed in water bath maintained at 60°C for 24 hours. Then, specimens were dried and brought to the testing temperature (25°C) and their initial weight ( $W_1$ ) was recorded (Plate 7.9). Finally, the testing was done similar to the specimens in dry Cantabro test and the average loss in weight is recorded (Plate 7.10). The weight loss was calculated according the Equation

$$CL = \frac{W_1 - W_2}{W_1} \times 100 \quad [7.5]$$

Where,  $W_1$  = Initial weight of specimen (g)

$W_2$  = Final weight of specimen (g)

$CL$  = Cantabro loss (%)

The lower the  $CL$ , higher is the ravelling resistance and vice versa.



Plate 7.9 Specimens before testing



Plate 7.10 Specimens after being tested

### 7.7.2 Analysis of Ravelling Resistance

The dry and wet Cantabro losses of the mixes are given in Figure 7.12 and 7.13, respectively. For all mixes, Cantabro weight losses of mixes after wet conditioning were found to be higher than dry conditioning, which indicated the loss of adhesion after conditioning of mixes in water (Figure 7.13). The wet Cantabro loss was found to increase with the filler content. The trend was found to be identical to that of moisture sensitivity, which might be due to the lowering of AFT with filler content. GP mixes suffered significantly higher losses (20-28%) after wet conditioning than GL, KS, and SD mixes (5-9%), which confirmed the negative influence of moisture on ravelling resistance of GP mixes.



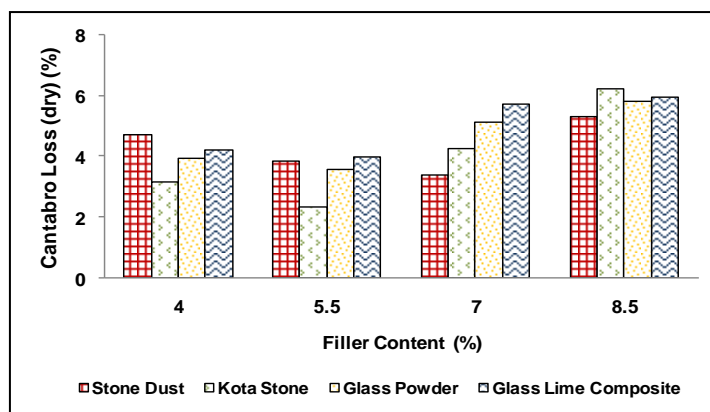


Figure 7.12 Variation of dry Cantabro loss of mixes with filler content

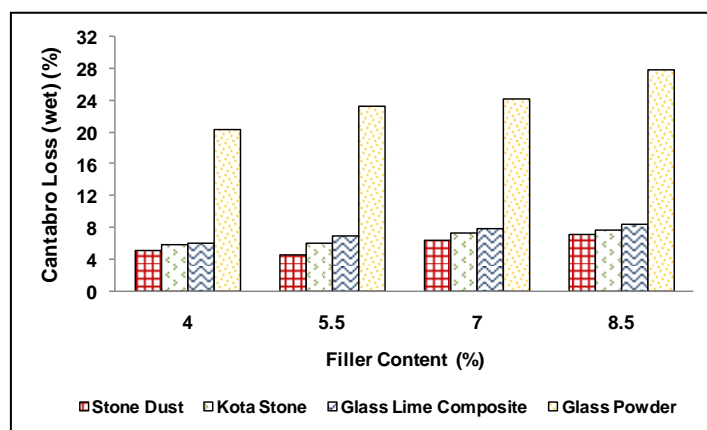


Figure 7.13 Variation of wet Cantabro loss of mixes with filler content

There is no well-defined trend for the dry Cantabro loss in the mixes. However, it seemed that in a dry state, losses decreased with an increase in filler content up to a limit and then marginal decline is observed at higher filler content. The decrease in Cantabro loss may be due to the stiffening of mastic with the addition of the filler in the mixes which might have increased the cohesion of mix. However, at higher filler contents, excessive stiffening and lower adhesion might have increased the losses.

For all mixes, Cantabro weight losses measured after wet conditioning are higher than dry conditioning, which indicated the loss of adhesion after conditioning of mixes in water. (Figure 7.13). This may be due to higher asphalt film thickness of these mixes or due to superior filler asphalt adhesion caused due to high dolomite composition in SD. In all mixes, wet Cantabro loss increased with the filler content in the mixes. In

dry conditioning, all mixes displayed good cohesion as all of them has a loss in weight less than 6%. No well defined trend observed for the dry Cantabro loss in the mixes. However it seemed that in dry state, losses decreased with increase in filler content up to a limit and then marginal decline is observed at higher filler content. Decrease in Cantabro loss may be due to the stiffening of mastic with the addition of the filler in the mixes which increased the impact resistance of the aggregates and that of the mixes (Kumari et al., 2018). However, at higher filler contents, excessive stiffening and lowering of OBC might have reduced the adhesion, which consequently has increased the losses. In contrast to results of wet Cantabro test, the losses in all mixes in dry state marginally differ from each other. Interestingly, GP and GL mixes displayed lower losses at lower filler contents (4 and 5.5%) than SD mixes. Hence, it can be said that although GP mixes displayed inferior performance in wet climatic conditions, they might perform satisfactorily in arid regions.

### **7.8 Long-Term Ageing Resistance**

During their service life, the bitumen and bituminous mixes observed hardening primarily due to oxidation of volatile components from the bitumen. This phenomenon is known as long-term ageing, and it influences the physical characteristics of the bituminous mixes and their performance against various distresses. Excessive hardening can also reduce the adhesion between the bitumen and aggregate, which increases the possibility of distresses like moisture damage and cracking. Hence ageing itself is not distress; instead, it can act as a catalyst for the other pavement distresses. It is desirable for a good quality mix to remain unaffected with the surrounding environmental conditions and maintain its premium properties throughout its service life.

The ageing susceptibility of the bituminous mixes can be determined using Ageing Index (AI), which is the ratio of the specific property of a mix in aged condition to that un-aged condition. It specifies the resistance of bituminous mix to permanent variation after being exposed to ageing conditions. Bituminous mixes having AI close to unity indicate higher ageing resistance of the mixes and vice versa (Kumari et al., 2019; Masoudi et al., 2017). In this study, AI of various bituminous mixes was calculated in terms of five different properties of bituminous mixes (Marshall stability, Marshall Quotient, indirect tensile strength, tensile strength ratio, and Cantabro loss (dry)).

### 7.8.1 Ageing Indices

There are several protocols to simulate long-term field ageing in the compacted bituminous mixes, which were already discussed in Chapter 2. However, in this study the field ageing was simulated according to AASHTO R30 protocol by conditioning the compacted specimen at a fixed temperature of 85°C for 5 days. The ageing indices in terms of various properties were determined using the Equations below.

$$AI = \frac{MS_{LTA}}{MS_{UA}} \quad [7.6]$$

$$AI = \frac{MQ_{LTA}}{MQ_{UA}} \quad [7.7]$$

$$AI = \frac{ITS_{LTA}}{ITS_{UA}} \quad [7.8]$$

$$AI = \frac{TSR_{LTA}}{TSR_{UA}} \quad [7.9]$$

$$AI = \frac{CL_{LTA}}{CL_{UA}} \quad [7.10]$$

Where, *LTA* and *UA* indicated the results of long-term and un-aged specimens respectively. *MS*, *MQ*, *ITS*, *TSR*, and *CL* represented Marshall stability, Marshall Quotient, indirect tensile strength, tensile strength ratio, and dry Cantabro loss of the mixes respectively. All parameters were calculated according to the protocols discussed in previous sections.

### 7.8.2 Analysis of Ageing Indices

The properties of various mixes subjected to short and long-term ageing are stated in Table 7.4, while various ageing indices are shown in Figures 7.14-7.18. At all filler contents, AI corresponding to MS, MQ, and ITS of mixes were found to be greater than unity. It was quite evident since bitumen tends to stiffen after being long aged which ultimately led to the increase in these properties of the mixes. Amongst these three indices, AI corresponds to MQ displayed higher than that corresponding to MS and ITS. Marshall quotient is the ratio of MS and flow at the failure. Hence it experienced highest increase since ageing of bitumen not only increased the stability of the mixes but also decreased the flow values, which resulted in higher increase in MQ. In general, AI of mixes corresponding to these properties increased with the filler content. This might be attributed to the decrease in AFT in the mixes because of lowering of OBC with increase in filler content. The mixes having lower AFT tends to oxidize faster which resulted in increased stiffening. In majority of the cases, GL mixes displayed highest AI, while SD mixes has the lowest AI. GL and SD mixes had the lowest and highest AFT, respectively that concur with the previous statement that ageing sensitivity of the mixes depends on their AFT.

In contrast of above mentioned AI's, the AI corresponds to TSR decreased with the increase in filler content. The AFT of the mixes and mineralogical composition of filler tends to affect the ageing sensitivity of the mixes. It was already established in previous sections that moisture resistance of bituminous mixes decreased with the AFT. Hence, AI of the mixes decreased with increase in filler content since mixes with lower AFT suffered higher hardening which also resulted in higher loss in TSR. GP mixes were found to be most ageing sensitive due to greater decline in TSR because of predominance of silica in GP, especially in mixes having higher filler contents (7 and 8.5%). On the other hand, SD and KS mixes didn't display any significant decline in TSR, and hence experienced a minor decline in AI.

Unlike the AI of previously discussed properties, trend of AI corresponding to CL was found to be very inconsistent. In previous section, it was observed that CL of mixes decreased with increase in stiffening of mastic. However excessive stiffening also found to reduce the adhesion in mastic that also increased the loss in mixes. Here it was observed that mixes having lower filler contents (4 and 5.5%), when being subjected to ageing tends to stiffen and led to lowering of CL, which also resulted in lowering of AI of their mixes. On the other hand, mixes prepared at higher filler contents exhibited excessive stiffening due to combined effect of higher filler content and oxidation of volatiles due to ageing. This resulted in increase of CL, which also resulted in increase of AI of their mixes. SD mixes displayed highest ageing sensitivity at mixes with 4% filler, while GL mixes displayed highest ageing sensitivity at mixes with 5.5, 7, and 8.5% filler. After comparison of AI corresponding to all properties, GL mixes seemed to be most ageing susceptible in majority of the

cases while conventional SD mixes are most ageing resistant. However this trend was not found synonymous to that of mastics and needed further studies in future.

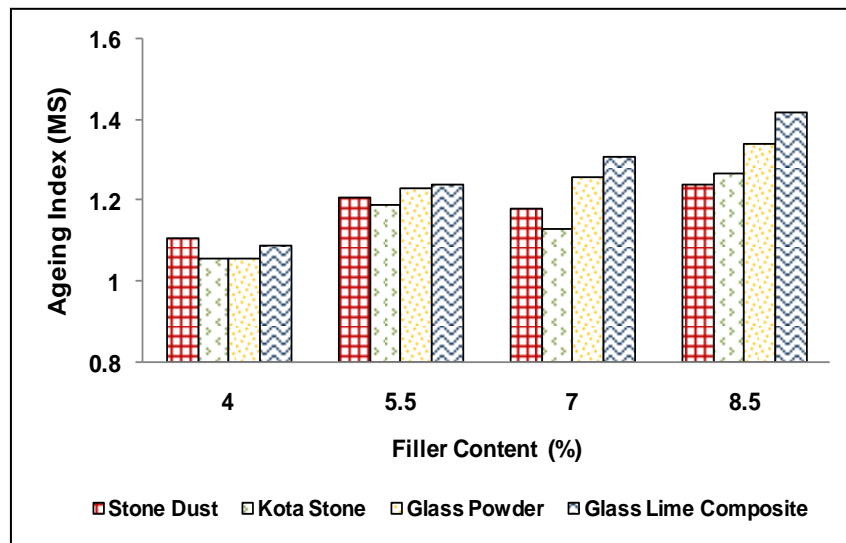


Figure 7.14 AI of various mixes corresponding to Marshall stability

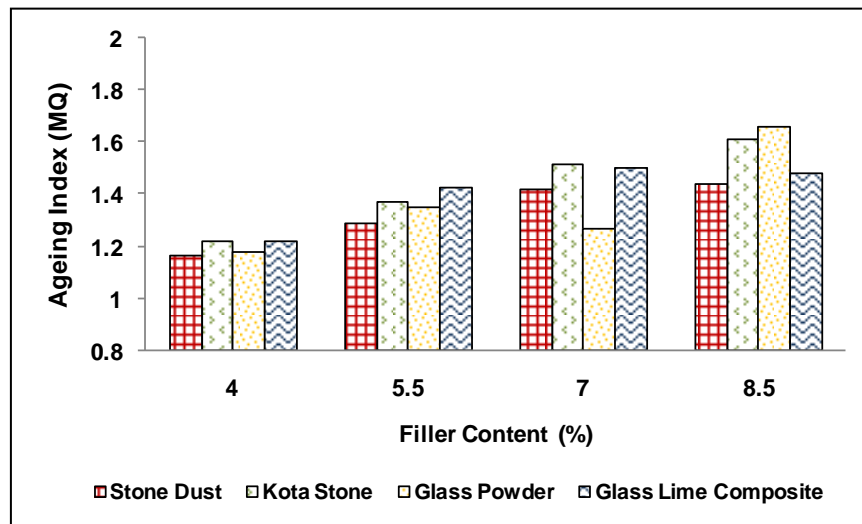


Figure 7.15 AI of various mixes corresponding to Marshall quotient

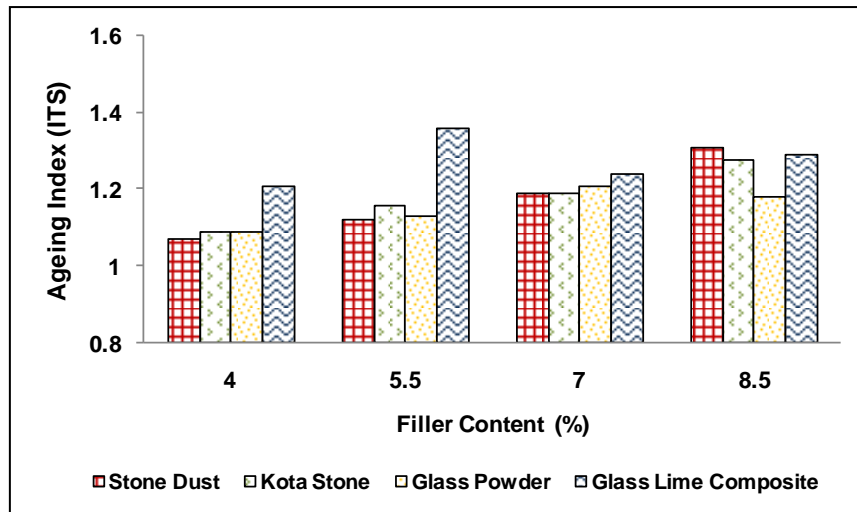


Figure 7.16 AI of various mixes corresponding to ITS

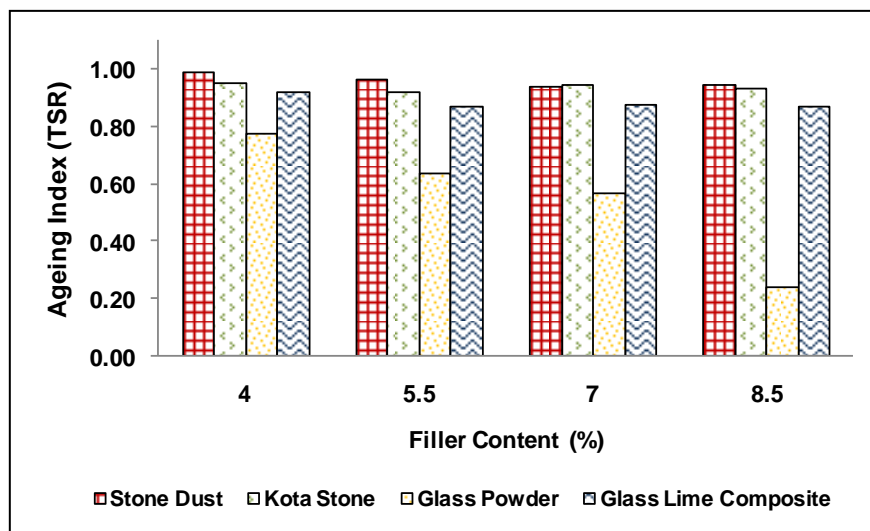


Figure 7.17 AI of various mixes corresponding to TSR

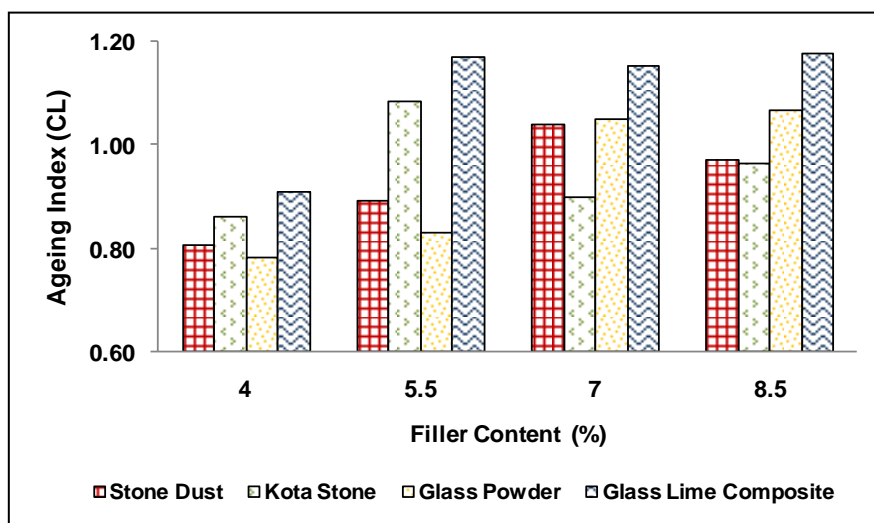


Figure 7.18 AI of various mixes corresponding to Cantabro loss

Table 7.4 Various properties of un-aged and long-term aged mixes

Property	Marshall stability (kN)		Marshall quotient (kN/mm)		Indirect tensile strength (kPa)		Cantabro loss (%)		Tensile strength ratio (%)	
	UA	LTA	UA	LTA	UA	LTA	UA	LTA	UA	LTA
Ageing condition										
Type of mix										
SD 4	12.22	13.56	3.57	4.18	652	698	4.74	3.83	94.23	93.22
SD 5.5	13.99	16.93	3.96	5.11	718	804	3.86	3.45	93.28	90.24
SD 7	15.96	18.83	4.57	6.49	851	1013	3.42	3.56	89.26	84.21
SD 8.5	16.58	20.56	5.16	7.43	948	1242	5.32	5.18	85.59	81.14
GP 4	12.98	13.76	3.85	4.54	727	792	3.94	3.08	54.05	42.12
GP 5.5	13.46	16.56	4.24	5.72	754	852	3.56	2.96	39.47	25.23
GP 7	14.93	18.81	4.66	5.92	892	1079	5.16	5.42	17.65	10.01
GP 8.5	14.52	19.46	4.93	8.18	972	1147	5.84	6.23	9.18	02.24
KS 4	12.65	13.41	3.77	4.60	684	746	3.16	2.72	93.82	89.22
KS 5.5	14.42	17.16	4.62	6.33	822	954	2.34	2.54	91.34	84.35
KS 7	15.61	17.63	5.29	8.04	949	1129	4.27	3.84	86.65	82.23
KS 8.5	16.34	20.75	5.64	9.08	996	1275	6.23	6.01	83.87	78.26
GL 4	14.32	15.61	4.45	5.43	826	999	4.22	3.84	88.58	81.65
GL 5.5	15.04	18.65	4.91	7.02	902	1227	4.00	4.68	85.34	74.12
GL 7	16.78	21.98	5.09	7.64	984	1220	5.75	6.64	81.12	71.11
GL 8.5	16.12	22.86	5.61	8.30	1038	1339	5.95	7.01	71.27	62.21

Note: UA = Un-aged; LTA= Long-term aged

## 7.9 Resilient Modulus

Resilient modulus ( $M_r$ ) is the most important input in flexible pavement design methodology because it signifies the capability of pavement layers to dispense load among them. It measures the responses of bituminous pavement layers towards the applied stresses and their corresponding strains (Akbulut et al., 2012; Arabani et al., 2017; Karami et al., 2018; Zoorab and Suparma, 2000). It is similar to the Young's modulus of bituminous mixes and an essential parameter used in structural analysis of pavements according to various mechanistic-empirical pavement design methods (AUSTROADS, 2010; French design manual, 1997; IRC 37, 2018). Although it is commonly measured using different methods (ASTM D 4123-82, 1995; ASTM D 7369-11, 2011; BS EN 12697-26, 2012), it is most commonly determined using



indirect tensile resilient modulus test. This is a non destructive test method, which is relatively simple, fast and its specimens can be easily prepared in laboratory. Similar to the ITFT test, testing of resilient modulus of various mixes is done in the pavement engineering laboratory of IIT (Kharagpur), India, whose details are specified below.



Plate 7.11 Setting up the test specimen



Plate 7.12 Close view of test setup

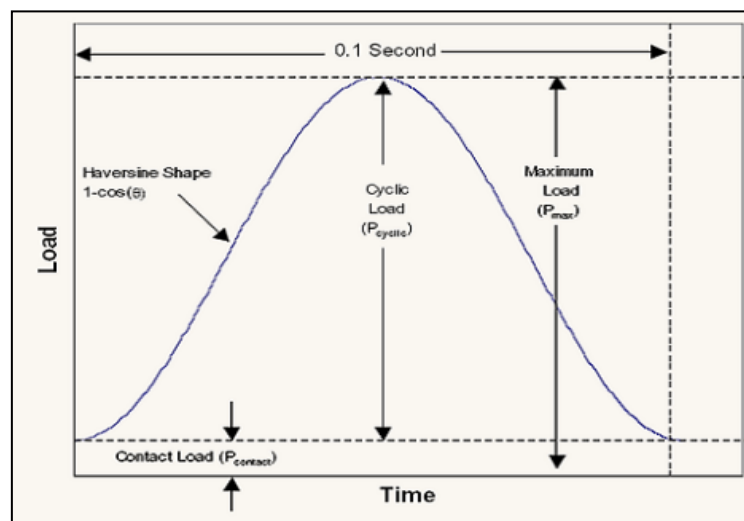


Plate 7.13 Haversine loading

### 7.9.1 Testing of Resilient Modulus

Resilient modulus of all mixes was determined by testing standard Marshall specimens (with 4% air voids) at indirect tensile mode as per ASTM D4123-82 (1995) guideline using UTM-14 machine (same as that used in ITFT test). The testing

was done at 25°C and 35°C. The machine was equipped with a temperature control chamber which maintains a constant temperature during specimen conditioning and testing. The chamber was also equipped with two linear variable differential transducers to measure the skin and core temperatures of the specimens (Plate 7.8 and 7.9). All specimens were conditioned in the chamber for 24 h to achieve targeted testing temperatures. A haversine load pulse was applied at a frequency of 1 Hz (0.1s load and 0.9s rest period) vertically along the vertical diameter of specimens using curved loading strips (Plate 7.10). The stress level in this test should lie in between 10-50% of the indirect tensile strength (ASTM D4123-82, 1995). Hence for each mix, the load corresponding to its 10% of ITS was used for testing. The horizontal deformation was determined using two linear variable differential transducers attached at the mid-thickness at the end of the horizontal diameter. Initially, each test specimen was conditioned by the application of 100 load pulses, and subsequently, the calculation of the modulus was done by taking the average of further five load pulses. The Poisson's ratio of each mix was assumed to be equal to 0.35 (Arabani et al., 2017; Modarres and Bengar 2017). For each mix, three samples were used, and every test was repeated two times, and average values are taken into consideration. The resilient modulus was calculated as per Equation 7.11:

$$M_r = \frac{P(\nu + 0.27)}{t\Delta\delta} \quad [7.11]$$

Where

$M_r$  = Resilient modulus (MPa),

$P$  = Applied load (N),

$\nu$  = Poisson's ratio,

$t$  = Thickness of the specimen (mm)

$\delta$  = Recoverable horizontal deformation (mm).

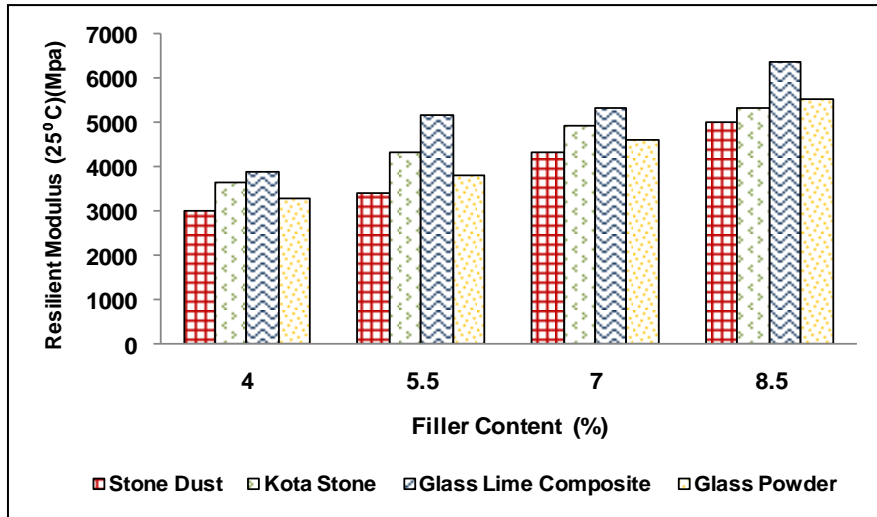


Figure 7.19 Variation of resilient modulus of mixes at 25°C with filler content

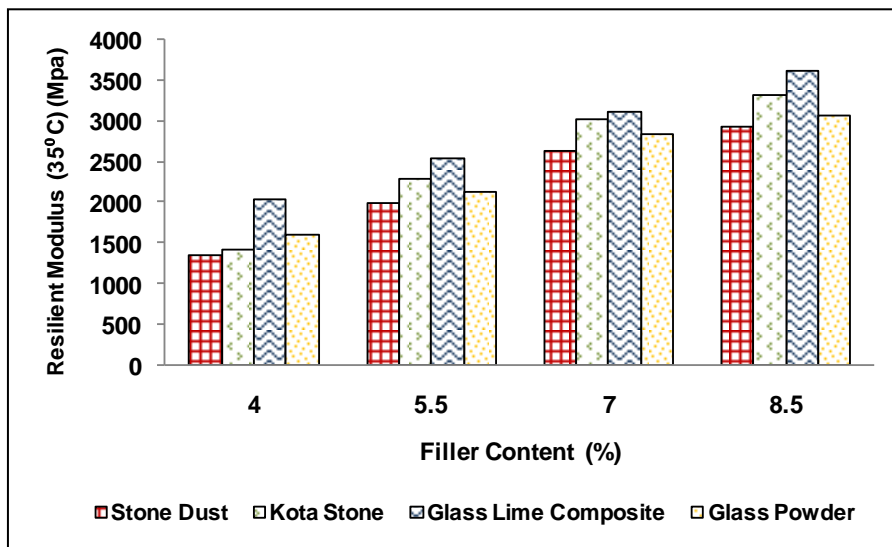


Figure 7.20 Variation of resilient modulus of mixes at 35°C with filler content

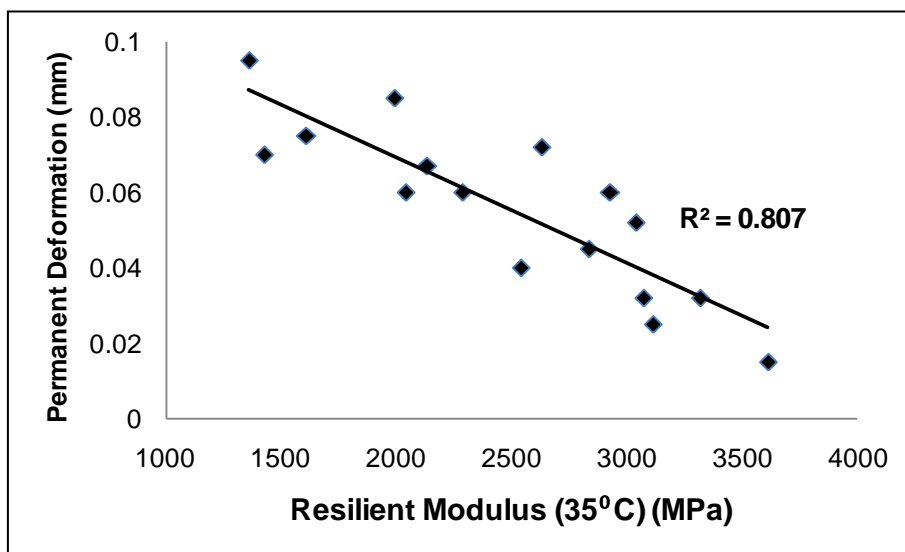


Figure 7.21 Relationship between resilient modulus and permanent deformation at 35°C

### 7.9.2 Analysis of Resilient Modulus

The  $M_r$  of various mixes determined at 25 and 35°C is stated in Figure 7.19 and 7.20, respectively. At both temperatures,  $M_r$  was found to increase with the increase in filler content.  $M_r$  indirectly represents the stiffness of the mixes and its load distribution ability. Since the stiffness of bituminous mixes was found to increase with filler content, this trend is justified. In all mixes, OBC was also decreased with an increase in filler content. Several studies (Akbulut et al., 2012; AGPT 02-10 2010; Hamzah and Yi, 2008) have also established that the  $M_r$  of bituminous mixes increases with the decrease in bitumen content. Although the trends of  $M_r$  at both temperatures were found to be similar, values at 25°C were found to be higher than at 35°C. This might be due to the lowering of elastic nature of bitumen at relatively higher temperature, which ultimately reduced the overall stiffness of the mixes. Conventional SD mixes were found to have lowest  $M_r$  values than mixes having waste fillers at each filler contents. It might be due to the lower OBC of waste filler modified mixes and due to the finer nature of filler particles in them. In general, it is believed that the use of finer fillers in the bituminous mixes resulting in their higher stiffness (Antunes et al., 2016; Liu et al., 2014; Modarres and Bengar, 2017). In general, GL mixes displayed highest  $M_r$  values followed by KS, GP, and SD mixes. Previous study (Diab and Enieb, 2018) has stated that the higher  $M_r$  is beneficial to improve the rutting resistance of the mixes. A good correlation between the permanent deformation (by static creep test) and  $M_r$  at 35°C was found, which validated the above statement (Figure 7.21). Hence,  $M_r$  analysis can also be done to determine the rutting resistance of the bituminous mixes. It can be said that mixes containing waste fillers exhibited superior load distribution capabilities than conventional mixes. Hence, flexible pavement layers

made with waste filler modified mixes might support similar traffic loading at a relatively lower layer thickness than conventional mixes.

## **7.10 Summary**

This chapter investigated the effect of type of filler and its quantity on the performance of bituminous mixes against various distresses. The mixes were prepared at their OBC, and their behavior was investigated using different protocols. The rutting resistance of various mixes was determined using Marshall quotient and uniaxial unconfined static creep and recovery test. It was observed that an increase in filler content in bituminous mixes tend to increase the rutting resistance of bituminous mixes. The improvement in rutting resistance was attributed to the lowering of VMA and AFT of the mixes. The rutting resistance parameters of bituminous mixes (MQ and permanent deformation) followed the trend synonymous to that of mastic parameters (Superpave rutting parameter and  $J_{nr}$  values). GL mixes were found to be the most rut resistant, followed by GP, KS, and conventional SD mixes.

The adhesion and moisture sensitivity of the bituminous mixes were found to be strongly dependent on the mineralogy of the fillers and AFT of the mixes. The moisture resistance of bituminous mixes was analyzed using modified Lottman and retained Marshall stability test. The moisture resistance of the bituminous mixes decreased with the increase in filler content due to the simultaneous lowering of AFT. The SD and KS mixes fillers exhibited superior performance against moisture due to presence of minerals like dolomite and calcite in the composition of respective fillers, which maintained strong bonding with bitumen even in the presence of water. GP mixes displayed abysmal performance against moisture due to predominance of silica

in the GP. Mixes prepared with GP failed to fulfill the minimum criteria of TSR. However, it was observed that up to 5% of GP can be used as filler after the addition of 2% of hydrated lime. Hydrated lime inhibited the moisture sensitive nature of GP and thus mixes with 7% GL (5% GP+ 2% lime) as filler delivered satisfactory moisture resistance. Active and passive adhesion of mixes were also exhibited the similar trends that of moisture sensitivity and found to decrease with the increase in filler contents.

Increase in filler content tends to increase the stiffness of the mixes, which also increased their ITS at 25°C and 0°C. It was also observed that the fineness and specific gravity of fillers influence the ITS of the mixes. In general, GL mixes displayed the highest ITS followed by KS, GP, and SD mixes at intermediate and low testing temperatures. The fatigue life of mixes was also determined at 25°C with ITFT test at stress controlled, mode and they were found to increase with filler content. GL mixes showed highest fatigue life followed GP, KS, and SD mixes. Good correlation was not found between the fatigue life of mixes and fatigue resistance of mastics determined using Superpave fatigue parameter and LAS tests. However, it was observed that fatigue life of mixes followed the similar trend as that of %R values obtained using MSCR test. It suggested that mode of testing significantly influence the fatigue behavior of the mastic and mixes.

Ravelling resistance of bituminous mixes was investigated using Cantabro test performed at standard conditions and after water immersion conditioning. Ravelling resistance of mixes was found to decrease with the increase in filler content and followed the trend similar to that of moisture sensitivity. However in the case of

standard testing, ravelling resistance was found to improve up to a certain filler content, and then slight decrease in resistance was observed. Significant difference between the results was not observed even in GP mixes, which suggested that it might be satisfactorily used in arid climates.

Long-term ageing sensitivity of the mixes in terms of its Marshall stability, MQ, ITS, TSR, and CL was determined by comparing the properties at aged and un-aged conditions. In majority of the cases, the ageing sensitivity of bituminous mixes was found to increase with increase in filler content. Bituminous mixes displayed highest ageing sensitivity against MQ and CL. Overall, GL and SD mixes displayed highest and lowest sensitivity towards ageing, respectively.

Finally, the load distribution behavior of the bituminous mixes at 25°C and 35°C was estimated with resilient modulus analysis using indirect tensile resilient modulus test. At both temperatures, resilient modulus of mixes improved with the higher filler proportion in the mixes. In majority of the cases, GL mixes displayed highest resilient modulus followed by KS, GP, and SD mixes. The resilient modulus was also found to decrease with the increase in testing temperatures. A good correlation between the resilient modulus and permanent deformation was also observed. It was inferred that mixes containing waste fillers might support similar traffic loading at a relatively lower layer thickness than conventional mixes. This aspect will be explored in the next sections of the study.